MOLECULAR AND CELLULAR BIOLOGY, Dec. 1994, p. 7967–7974
0270-7306/94/$04.00+0

Vol. 14, No. 12

NF-κB Sites Function as Positive Regulators of Expression of the Translocated c-*myc* Allele in Burkitt's Lymphoma

LIN JI, MAGDALENA ARCINAS, AND LINDA M. BOXER*

Center for Molecular Biology in Medicine, Palo Alto Veterans Administration Hospital, and Department of Medicine, Stanford University School of Medicine, Stanford, California 94305

Received 7 June 1994/Returned for modification 21 July 1994/Accepted 30 August 1994

An in vivo footprint over a potential NF-κB site in the first exon of the c-*myc* gene has been identified on the translocated allele in the Ramos Burkitt's lymphoma cell line. The potential NF-κB site in the 5′ flanking sequence of c-*myc* was found to be occupied on the translocated allele in the Raji Burkitt's cell line. Electrophoretic mobility shift assays with each of these sequences demonstrated complexes with mobilities identical to those of the NF-κB site from the κ light-chain gene. A supershift was obtained with anti-p50 antibody with the exon site. The upstream-site shift complex disappeared with the addition of anti-p50 antibody. Binding of NF-κB proteins to the c-*myc* exon and upstream sites was demonstrated by induction of binding upon differentiation of pre-B 70Z/3 cells to B cells. UV cross-linking experiments revealed that a protein with a molecular mass of 50 kDa bound to the exon and upstream sites. Transfection experiments with Raji cells demonstrated that both sites functioned as positive regulatory regions, with a drop in activity level when either site was mutated. Access to these sites is blocked in the silent normal c-*myc* allele in Burkitt's lymphoma cells, while Rel family proteins bind to these sites in the translocated allele. We conclude that the two NF-κB sites function as positive regulatory regions for the translocated c-*myc* gene in Burkitt's lymphoma.

Burkitt's lymphoma is associated with specific chromosomal alterations which juxtapose the c-*myc* gene to one of the immunoglobulin loci. These translocations deregulate the expression of c-*myc* such that the translocated c-*myc* allele is expressed at high levels and the normal allele is usually silent (3, 11, 19, 28). Although the mechanism of the deregulation of c-*myc* is unknown, regulatory elements of the immunoglobulin locus may play a role. Other findings that may be involved include alternative promoter preference in the translocated allele (6, 37), relief of a block to transcription elongation in the translocated allele (7, 15, 27), and somatic mutations in the 3′ region of exon I and the 5′ region of intron I (8, 30, 40, 41). The mutations in this region may disrupt a negative regulatory element.

The deregulated c-*myc* gene is believed to play a role in the pathogenesis of Burkitt's lymphoma. Transgenic mice which carried the c-*myc* gene linked to the immunoglobulin intron enhancer developed B-cell malignancies (1, 29). Furthermore, when lymphoblastoid cells immortalized by Epstein-Barr virus were transfected with a constitutively expressed c-*myc* gene, the cells became tumorigenic in nude mice (24).

NF-κB is an inducible transcription factor involved in the activation of many genes in different cell types (5). The consensus binding sequence for NF-κB is GGGR(C/A/T)TYYCC. Different combinations of the Rel family proteins bind as dimers to NF-κB sites. Classical NF-κB is a heterodimer of p50 and p65; the p65 subunit binds to the 3′ side of the NF-κB site. Two functional NF-κB sites have been identified within the murine c-*myc* gene (12, 21, 22). One of the NF-κB sites in the murine c-*myc* gene differs from the consensus sequence in that it contains only T residues in the 3′ pyrimidine stretch (21), and classical NF-κB has been shown to transactivate the murine c-*myc* promoter while c- and v-Rel do not (22).

We are studying in vivo protein binding to the two c-*myc* alleles in Burkitt's lymphoma cell lines. We identified an in vivo footprint at a potential NF-κB site in the first exon of the translocated c-*myc* allele. This corresponds to the location of the NF-κB site in the murine c-*myc* gene. In addition, we located an in vivo footprint over the upstream NF-κB site on the translocated c-*myc* allele. We demonstrated that Rel family proteins bind to these sites in vitro and that mutation of these sites decreased c-*myc* expression in the Raji Burkitt's cell line. Our results suggest that these sites function as positive regulatory elements for the translocated c-*myc* allele in Burkitt's lymphoma.

MATERIALS AND METHODS

Cell lines. DHL-9 is a B-cell line which does not contain a translocation of the c-*myc* gene; Raji and Ramos are Burkitt's lymphoma cell lines. Cells from these three lines were grown in RPMI medium with 10% fetal bovine serum. 70Z/3 cells were grown in RPMI medium with 10% fetal bovine serum and 50 μM 2-mercaptoethanol. Phorbol 12-myristate 13-acetate at 25 ng/ml was added to induce differentiation. Nuclear extracts were prepared after exposure to phorbol 12-myristate 13-acetate for 2 h.

Plasmid constructs. pMPCAT (4), which contains c-*myc* residues −2328 to +936, was obtained from D. Levens (National Institutes of Health). Mutations were created in the NF-κB sites by PCR mutagenesis (20). The primers used were GCCCATTTGGCCACACTT (c-*myc* exon site) and GGAG CACAAGCCTCTCTG (c-*myc* upstream site) (the mutated bases are underlined). Mutations were confirmed by sequencing (Sequenase kit; U.S. Biochemicals).

In vivo DMS treatment and DNA isolation. Cells (10^8) were washed twice in phosphate-buffered saline (PBS) and resuspended in 1 ml of medium (RPMI medium with 10% fetal bovine serum) with 0.005% dimethyl sulfate (DMS). After

* Corresponding author. Mailing address: Division of Hematology, S-161, Stanford University School of Medicine, Stanford, CA 94305-5112. Phone: (415) 493-5000, ext. 3126. Fax: (415) 858-3986.

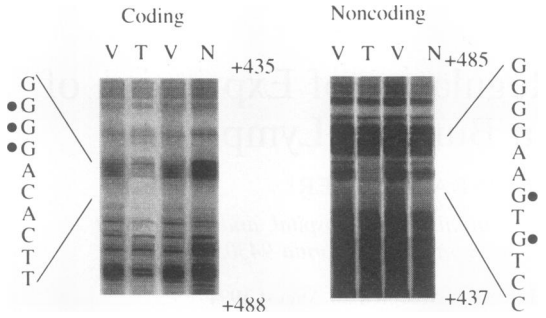

FIG. 1. In vivo footprint analysis by LMPCR of the c-*myc* exon NF-κB site in Ramos cells. The regions illustrated are labeled with nucleotide numbers relative to the c-*myc* P1 promoter. Lanes (from left to right for both gels): V, in vitro-methylated DNA from the translocated c-*myc* allele; T, in vivo-methylated DNA from the translocated c-*myc* allele: V, in vitro-methylated DNA from the normal c-*myc* allele; N, in vivo-methylated DNA from the normal c-*myc* allele. The protected guanines are indicated by closed circles. Protection of guanine for the coding strand is 72% at position +460, 69% at +461, and 66% at +462. Protection for the noncoding strand is 75% at +464 and 54% at +466.

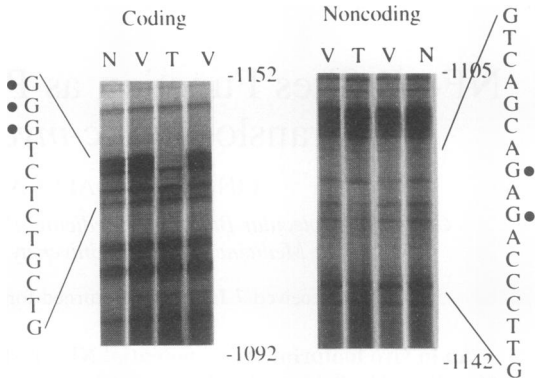

FIG. 2. In vivo footprint analysis by LMPCR of the c-*myc* upstream NF-κB site in Raji cells. The lanes are labeled as in Fig. 1. Protection of guanine for the coding strand is 65% at position −1130, 74% at −1129, and 27% at −1128. Protection for the noncoding strand is 83% at −1126 and 71% at −1124.

incubation for 5 min at room temperature, the cells were washed in medium without DMS and were then washed with PBS. The nuclei were isolated as described by Wijnholds et al. (39). DNA was isolated from nuclei as described previously (34) or by the use of the Qiagen cell culture DNA kit. The DNA was digested with *Sac*I for Raji cells and with *Bgl*II for Ramos cells. Agarose gel electrophoresis was performed to separate the translocated c-*myc* allele from the normal one. One lane of the gel was transferred to a filter; probes consisting of c-*myc* exons 2 and 3 and the immunoglobulin μ heavy-chain constant region were used sequentially to locate the two c-*myc* alleles. The DNA in these two regions was electroeluted from the gel. Cleavage with piperidine was performed according to the Maxam-Gilbert procedure (25). The sizes of fragments obtained after chemical cleavage were checked on an agarose gel; the average fragment size was usually 200 to 300 bp.

In vitro DMS treatment. Control samples of genomic DNA were subjected to DMS treatment in vitro followed by piperidine cleavage. Genomic DNA was prepared as described above without prior DMS treatment. Genomic DNA (50 μg) was treated with 0.24% DMS for 1 min at room temperature and then treated as described by Maxam and Gilbert (25). Separation of the translocated and normal alleles was performed as described above. To provide a more complete sequence, DNA was also chemically modified and cleaved by the standard G+A Maxam-Gilbert chemistry.

LMPCR. Chemically modified and cleaved DNA was then subjected to amplification by ligation-mediated PCR (LMPCR) essentially as described by Mueller and Wold (26), Pfeifer et al. (31), and Garrity and Wold (16). Sequenase was used for first-strand synthesis, and *Taq* DNA polymerase was used for PCR. Conditions used for amplification were 95°C for 2 min, 61°C for 2 min, and 76°C for 3 min. After 20 to 22 cycles of PCR, samples were hybridized with end-labeled primers (the third primer of each primer set) and amplified by one more cycle of PCR. The reaction mixtures were resolved in a 6% polyacrylamide denaturing gel. Footprinting on each strand was repeated at least four times with genomic DNA samples prepared from at least three separate batches of DMS-treated cells. The primers used for PCR were synthesized in an Applied Biosystems 380B DNA synthesizer and purified on Applied Biosystems oligonucleotide purification cartridges. The common linkers used were GCGGTGACCC GGGAGATCTGAATTC and GAATTCAGATC. The exon primers for the coding strand were AAAAGGCAAGTGGA CTTCGGTGCT, GACTTCGGTGCTTACCTGGTTTTCC, and TTCGGTGCTTACCTGGTTTTCCACTAC; the up stream primers were TCAAAGGTGCTAGACGGGAGAAT ATG, AGAATATGGGAGGGGCAGGGGGTAC, and AAT ATGGGAGGGGCAGGGGGTACCCGAAC. The exon primers for the noncoding-strand were CCTTGCCGCATC CACGAAAC, CGAAACTTTGCCCATAGCAGCGGG, and AACTTTGCCCATAGCAGCGGGCGG; the upstream primers were CGCATTTCCAATAATAAAAGGGGAAAGAG, AGGGGAAAGAGGACCTGGAAAGG, and GGAAAGAG GACCTGGAAAGGAATTAAACGTCC. Quantitation of footprints was performed as described previously (2) with ImageQuant software, version 3.15 (Molecular Dynamics). Percent protection values below 20% were considered too low and were not interpreted as footprints.

EMSA. The sequences of the oligonucleotides used for the electrophoretic mobility shift assay (EMSA) are as follows (the NF-κB sites are underlined): GAGGCA<u>GGGACTTTCC</u>TGT CCC (human immunodeficiency virus–κ light-chain gene [HIV-κ]) GAGGTG<u>GGGACACTTC</u>CCTCCC (c-*myc* exon), and GAGGAA<u>GGGTCTCTGC</u>TGTCCC (c-myc upstream). Oligonucleotides with the mutations described above in the c-*myc* upstream and exon sites were also labeled and used in the EMSA. The oligonucleotides were synthesized with 5′ overhangs and end labeled with [α-^{32}P]dCTP and Klenow. The binding solution was as follows: 12 mM HEPES (*N*-2-hydroxyethylpiperazine-*N*′-2-ethanesulfonic acid) (pH 7.9), 4 mM Tris (pH 7.5), 100 mM KCl, 1 mM EDTA, 1 mM dithiothreitol, 12% glycerol, 2 μg of poly(dI-dC), 1 μg of bovine serum albumin (BSA), 0.5 ng (10^4 cpm) of end-labeled DNA oligonucleotide probe, and 15 to 20 μg of protein from crude nuclear extract. The binding reaction was conducted at room temperature for 15 min, and the samples were loaded onto a 0.5× Tris-borate-EDTA–5% polyacrylamide gel. Electrophoresis was performed at 30 mA at 4°C. For the competition studies, various molar excesses of an unlabeled competitor oligonucleotide were added to the binding reaction mixture. As a nonspecific competitor, an oligonucleotide containing the Myb binding site was used: AATTAACTGCTTAACTGTC AA. For the supershifts, the binding reaction was performed as

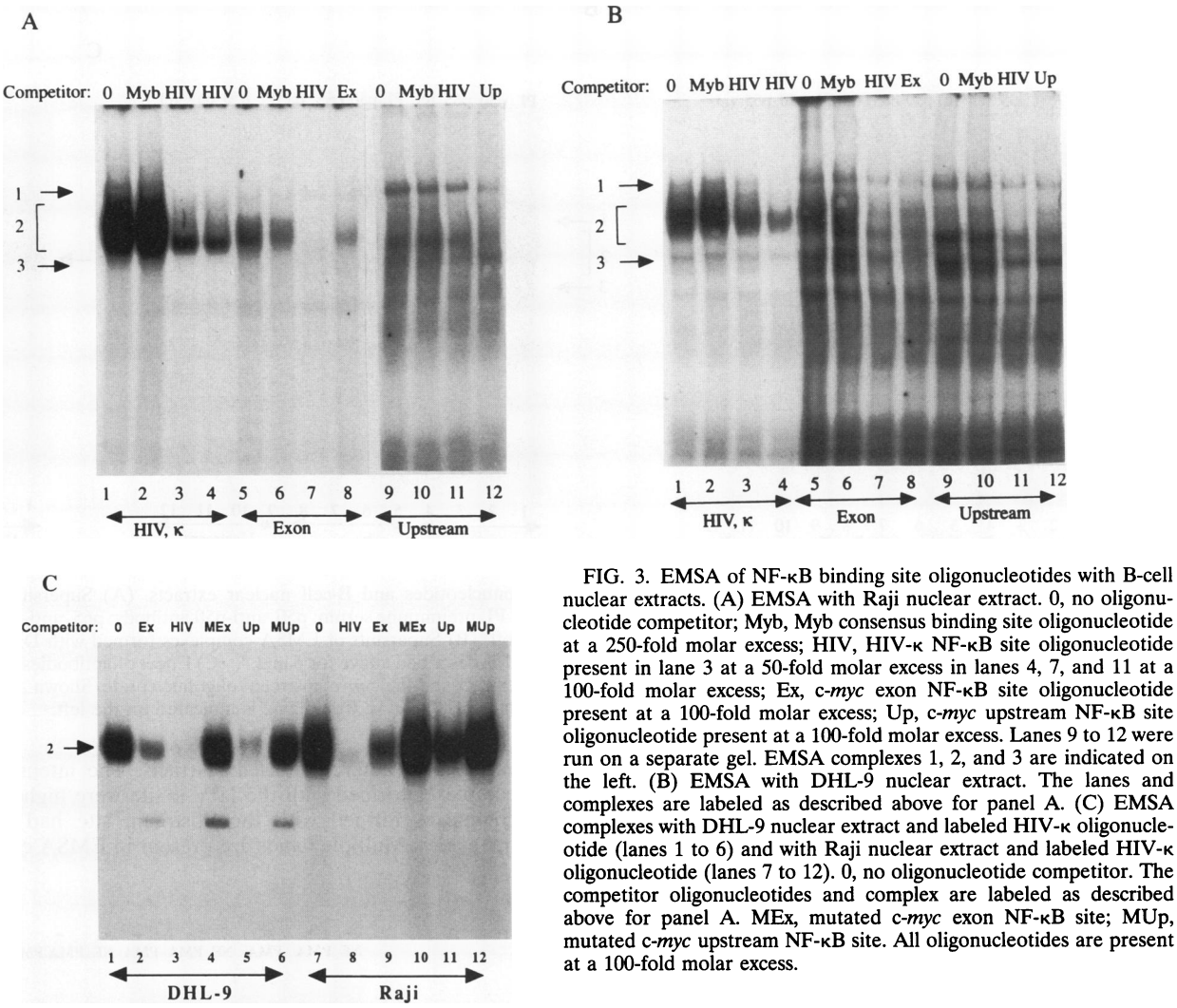

FIG. 3. EMSA of NF-κB binding site oligonucleotides with B-cell nuclear extracts. (A) EMSA with Raji nuclear extract. 0, no oligonucleotide competitor; Myb, Myb consensus binding site oligonucleotide at a 250-fold molar excess; HIV, HIV-κ NF-κB site oligonucleotide present in lane 3 at a 50-fold molar excess in lanes 4, 7, and 11 at a 100-fold molar excess; Ex, c-*myc* exon NF-κB site oligonucleotide present at a 100-fold molar excess; Up, c-*myc* upstream NF-κB site oligonucleotide present at a 100-fold molar excess. Lanes 9 to 12 were run on a separate gel. EMSA complexes 1, 2, and 3 are indicated on the left. (B) EMSA with DHL-9 nuclear extract. The lanes and complexes are labeled as described above for panel A. (C) EMSA complexes with DHL-9 nuclear extract and labeled HIV-κ oligonucleotide (lanes 1 to 6) and with Raji nuclear extract and labeled HIV-κ oligonucleotide (lanes 7 to 12). 0, no oligonucleotide competitor. The competitor oligonucleotides and complex are labeled as described above for panel A. MEx, mutated c-*myc* exon NF-κB site; MUp, mutated c-*myc* upstream NF-κB site. All oligonucleotides are present at a 100-fold molar excess.

described above with incubation for 15 min at room temperature. Antibody was added, and the incubation was continued for 1 h at 4°C. The polyclonal antibodies against p50, p65, c-Rel, Sp-1, wt-1, and egr-1 were obtained from Santa Cruz Biotechnology.

UV cross-linking and SDS-polyacrylamide gel electrophoresis. The EMSA was performed as described above. The wet gel was exposed to film to locate the EMSA complexes. UV cross-linking was performed essentially as described previously (9) with a short-wavelength UV light box at 4°C for 30 min. Regions of the gel containing the complexes were cut out, and the individual complexes were eluted at room temperature overnight in 50 mM Tris-HC1 (pH 7.9)–0.1% sodium dodecyl sulfate (SDS)–0.1 mM EDTA–5 mM dithiothreitol–150 mM NaC1–0.1 mg of BSA per ml. The eluted protein was precipitated with 4 volumes of acetone, washed with ethanol, and air dried. After resuspension in Laemmli loading buffer, SDS-polyacrylamide gel electrophoresis was performed. The Amersham ECL kit was used for Western (immunoblot) analysis.

Transfections and CAT assays. Transfections were performed with cells in log phase. Cells were washed and resuspended in unsupplemented RPMI medium to a final concentration of 2×10^7 cells per ml and incubated for 10 min at room temperature after the addition of 15 μg of DNA plus 10 μg of DEAE-dextran (17). Electroporations were carried out with the Bio-Rad gene pulser at 350 mV and 960 μF. The cells were then incubated again for 10 min at room temperature. Transfected cells were cultured in 23 ml of supplemented RPMI medium for 48 h. Chloramphenicol acetyl-transferase (CAT) assays were performed in the standard manner (18) with a 2-h enzyme assay. Percent acetylation was quantified by cutting out sections of the thin-layer chromatography plate that corresponded to the acetylated and unacetylated forms; this step was followed by scintillation counting, or quantification was performed by use of a Molecular Devices phosphorimager. Variations in transfection efficiency were controlled for by cotransfection with Rous sarcoma virus-β-galactosidase. Each assay was performed at least three times in duplicate with at least two different plasmid preparations. The average values with the standard deviations are plotted (see Fig. 7B).

RESULTS

An in vivo footprint is located in exon I at a potential NF-κB site. The translocation breakpoint in Ramos cells is located 340 bp 5′ of the c-*myc* gene. The translocated and normal c-*myc* alleles from Ramos cells were separated by electrophoresis, and LMPCR was performed on each one. With primer sets

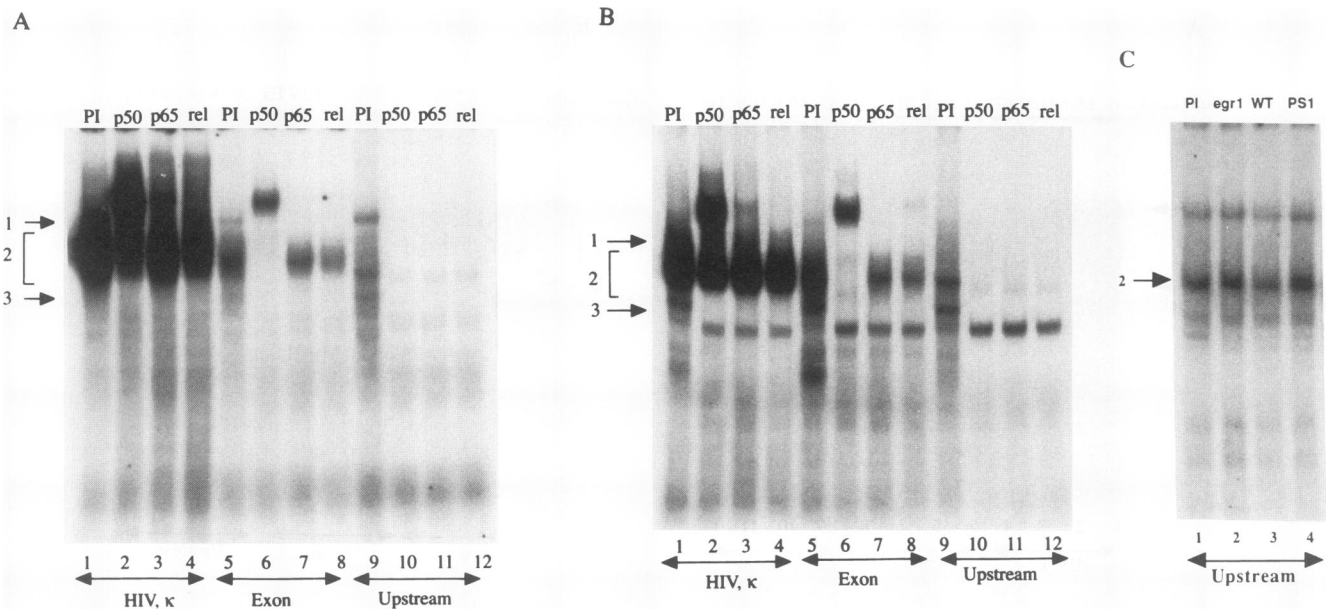

FIG. 4. Supershift of EMSA complexes formed with the NF-κB oligonucleotides and B-cell nuclear extracts. (A) Supershift of EMSA complexes formed with Raji nuclear extract and the NF-κB oligonucleotides. PI, preimmune serum; p50, anti-p50 antibody; p65, anti-p65 antibody; rel, anti-Rel antibody. EMSA complexes 1, 2, and 3 are indicated on the left. (B) Supershift of EMSA complexes formed with DHL-9 nuclear extract and the NF-κB oligonucleotides. The lanes and complexes are labeled as described above for panel A. (C) Effect of antibodies against other transcription factors on the EMSA complexes formed with DHL-9 nuclear extract and the c-*myc* upstream oligonucleotide. Shown are the effects of the addition of PI (lane 1), anti-egr-1 (lane 2), anti-wt-1 (lane 3), and anti-Sp-1 (lane 4). Complex 2 is indicated on the left.

that cover a region of the 3′ end of exon I, we found a footprint on the translocated c-*myc* allele which was not present on the normal silent c-*myc* allele (Fig. 1). Three guanine residues were protected on the coding strand, and two guanine residues demonstrated protection on the noncoding strand. The protected sequence is similar to the NF-κB consensus binding sequence, with two residues (shown in bold) differing from those of the consensus sequence: GGGACACTTC. (See Fig. 7A for the locations of the NF-κB sites in the c-*myc* promoter.)

The upstream NF-κB site is protected in vivo in Raji cells. A potential NF-κB element is located in the upstream region of the human c-*myc* gene. This region is located on a different chromosome from that of the translocated c-*myc* gene in Ramos cells, while the 3′ region of the first exon (including the exon NF-κB site) is deleted in Raji cells. To determine whether proteins bind in vivo to the upstream NF-κB site, LMPCR was performed with primers to cover this site in Raji cells. A protected region was located on the translocated c-*myc* allele but not on the normal allele (Fig. 2). Three guanine residues were protected on the coding strand, and two guanine residues were protected on the noncoding strand. This sequence differs from the NF-κB consensus binding sequence by two bases (shown in bold): GGG**T**CTCT**G**C. One of the mismatched bases is located in the 3′ pyrimidine string.

Rel family proteins bind to the c-*myc* sites in vitro. The protected sequences are not perfect matches to the NF-κB site, so we wished to determine whether Rel family proteins could bind to these sites. EMSA was performed with the c-*myc* exon and upstream NF-κB sites, and the HIV-κ NF-κB sequence was used as a positive control. Nuclear extracts were prepared from DHL-9 B cells, which do not contain a translocation involving c-*myc*, and from Raji Burkitt's lymphoma cells. Three complexes with similar mobilities were formed with oligonucleotides of all three sites with nuclear extracts from both cell lines (Fig. 3A and B). The amounts of complexes 1 and 3 varied with different nuclear extracts. The intensities of the complexes formed with the HIV-κ site were highest, and the complexes formed with the upstream site had the lowest intensities. Multiple bands are present in EMSA complex 2 of

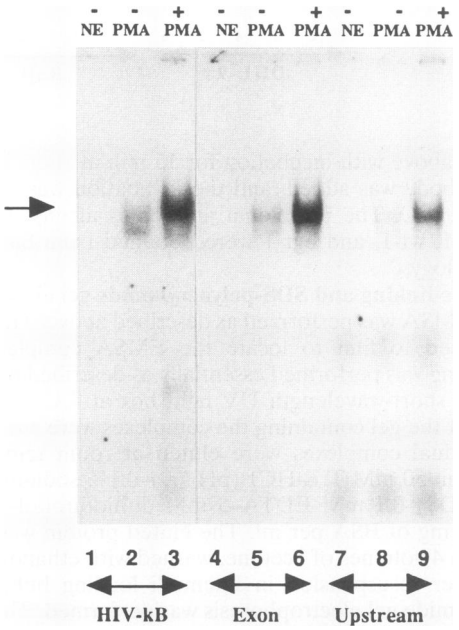

FIG. 5. EMSA complexes formed with differentiated 70Z/3 cells. Lanes 1, 4, and 7 demonstrate the mobility of a free probe without the addition of nuclear extract (NE). Lanes 2, 5, and 8 contain nuclear extract prepared from undifferentiated 70Z/3 cells. Lanes 3, 6, and 9 contain nuclear extract from differentiated 70Z/3 cells. PMA, phorbol 12-myristate 13-acetate. Complex 2 is indicated by the arrow.

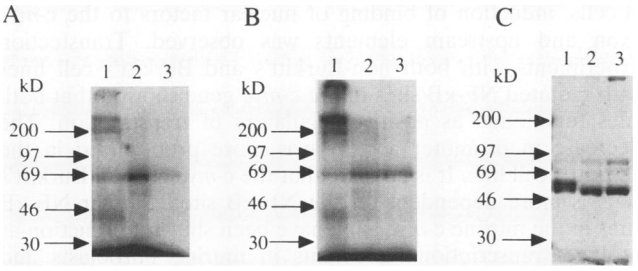

FIG. 6. Determination of the molecular sizes of the proteins that bind to the c-*myc* NF-κB sites. (A) Denaturing SDS-polyacrylamide gel analysis of the UV cross-linked EMSA complexes formed with the c-*myc* exon NF-κB site and DHL-9 nuclear extract. Lanes 1, 2, and 3 contain the proteins found in EMSA complexes 1, 2, and 3, respectively. The migration of the molecular weight markers is shown on the left. When the migration is corrected for the bound oligonucleotide sequences, the molecular mass of the major protein in lanes 1 to 3 is 50 kDa. (B) Denaturing SDS-polyacrylamide gel analysis of the UV cross-linked EMSA complexes formed with the c-*myc* upstream NF-κB site and DHL-9 nuclear extract. The lanes are labeled as described above for panel A. (C) Western analysis with anti-p50 antibody of the noncross-linked EMSA complexes formed with the c-*myc* exon NF-κB site and DHL-9 nuclear extract. When Western analysis is performed with UV cross-linked EMSA complexes, the band on the Western blot comigrates with the major ^{32}P-labeled band shown in panel A.

the HIV-κ site and the c-*myc* exon sites, while the c-*myc* upstream site yields only the fastest-migrating band. Competition with excess cold oligonucleotides demonstrated that the HIV-κ element competed against both the c-*myc* exon and the upstream sites (Fig. 3A and B). The c-*myc* exon and upstream elements also competed against the HIV-κ sequence (Fig. 3C). The two c-*myc* sites competed against each other, as well (data not shown).

Antibodies against p50, p65, and c-Rel were used in the EMSA to determine whether any of these proteins were in the gel shift complexes. As expected, both anti-p50 and anti-p65 supershifted the complex formed with the HIV-κ site (Fig. 4A and B). The complex formed with the c-*myc* exon site was supershifted with anti-p50 and to a lesser extent with anti-c-Rel (Fig. 4A and B). All three antibodies caused the complex formed with the c-*myc* upstream site to disappear, but no supershift was observed (Fig. 4A and B). These antibodies had no effect on complexes formed with either a c-Myb or Sp-1 binding site; there was no effect of the antibodies on the migration of the c-*myc* upstream sequence in the absence of nuclear extract (data not shown). Antibodies against several proteins not related to the Rel family had no effect on the EMSA complex formed with the c-*myc* upstream sequence (Fig. 4C).

Treatment of 70Z/3 pre-B cells with lipopolysaccharide or phorbol 12-myristate 13-acetate results in differentiation to a B cell. Activation of NF-κB binding and induction of κ light-chain synthesis occur during differentiation (35). Treatment of 70Z/3 cells with phorbol 12-myristate 13-acetate for 2 h induced binding to the HIV-κ site, the c-*myc* exon site, and the c-*myc* upstream site (Fig. 5). These EMSA complexes had the same mobility as complex 2 in the EMSAs with these oligonucleotides and DHL-9 or Raji nuclear extract.

To confirm that Rel family proteins bind to the c-*myc* exon and upstream sites, UV cross-linking followed by denaturing polyacrylamide gel electrophoresis was performed. A major protein with a molecular mass of 50 kDa was observed in association with all three exon complexes (Fig. 6A) and with

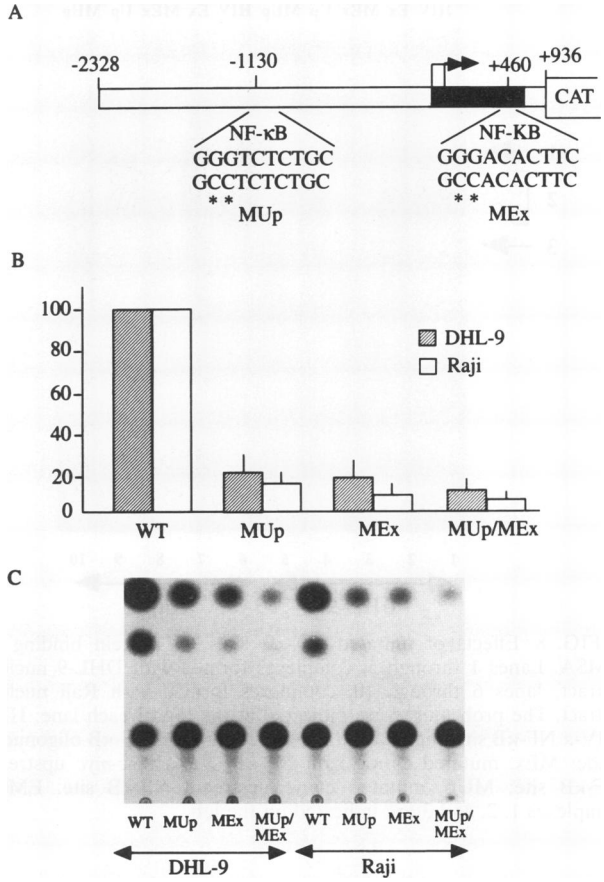

FIG. 7. Effect of mutated NF-κB sites on c-*myc* promoter activity. (A) Diagram of c-*myc* promoter-CAT construct used for transfection experiments. The locations of the two NF-κB sites are indicated, and the sequences of the mutant sites (MUp and MEx) are also shown (asterisks indicate mutated nucleotides). (B) Transient transfection analyses of c-*myc* promoter-CAT constructs. WT, wild-type c-*myc* promoter construct; MUp, mutant upstream NF-κB construct; MEx, mutant exon NF-κB construct; MUp/MEx, double mutant. *y* axis, relative CAT activities. (C) Representative CAT assay.

the upstream complexes (Fig. 6B). There were also two larger proteins present in complex 1; these have not been further characterized.

The identity of the protein present in these complexes was also analyzed by Western blotting. Similar results were obtained whether the DNA probe was cross-linked to the protein or not. The results of Western analysis with the anti-p50 antibody of the exon complexes in the absence of UV cross-linking are shown in Fig. 6C. The anti-Rel antibody showed very faint staining with all three exon complexes, which is consistent with the supershift results, while little if any p65 was observed (data not shown). Similar results were obtained with the upstream complexes (data not shown).

The NF-κB sites demonstrate functional activity in B cells. The c-*myc* promoter is active in both DHL-9 and Raji cells. To determine whether the protected sequences have any functional activity, mutations were introduced into each NF-κB site (Fig. 7A). By EMSA, protein binding to the mutated sequences was dramatically decreased (Fig. 8); the mutated sequences did not compete against the EMSA complexes formed with the HIV-κ element (Fig. 3C). Mutation of the exon site decreased the activity of the c-*myc* promoter by 88%

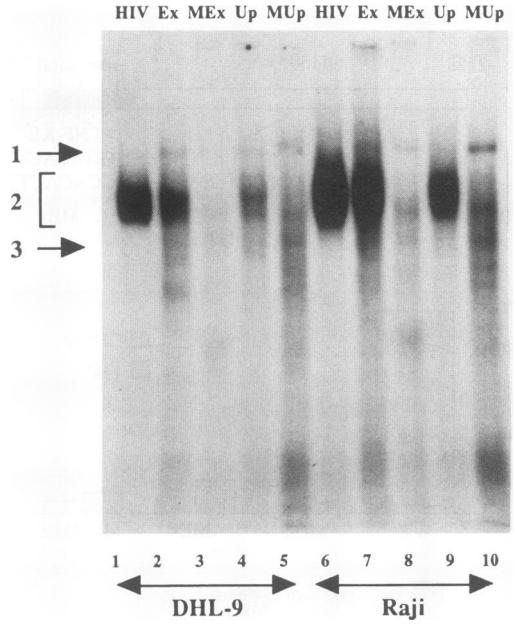

FIG. 8. Effects of mutated NF-κB sites on protein binding by EMSA. Lanes 1 through 5, complexes formed with DHL-9 nuclear extract; lanes 6 through 10, complexes formed with Raji nuclear extract. The probes used are indicated at the top of each lane: HIV, HIV-κ NF-κB site oligonucleotide; Ex, c-*myc* exon NF-κB oligonucleotide; MEx, mutated c-*myc* exon NF-κB site; Up, c-*myc* upstream NF-κB site; MUp, mutated c-*myc* upstream NF-κB site. EMSA complexes 1, 2, and 3 are indicated on the left.

in Raji cells. The decrease in activity was somewhat less in DHL-9 cells (81%) (Fig. 7B and C). There was also a substantial drop in activity with mutation of the upstream site, 84% in Raji cells and 79% in DHL-9 cells (Fig. 7B and C). Mutation of both sites simultaneously decreased the c-*myc* promoter activity by 91% in Raji cells and by 86% in DHL-9 cells (Fig. 7B and C).

DISCUSSION

We have used in vivo footprinting to identify two regions which are protected in vivo on the translocated c-*myc* allele in Burkitt's lymphoma cells. The normal c-*myc* allele, which is transcriptionally silent, does not show any protection in these areas. The locations of these sites correspond to the locations of NF-κB sites in the murine c-*myc* gene (21, 22). Although these sites differ slightly from those of the consensus NF-κB binding sequence, we have demonstrated by several criteria that Rel family proteins bind to these sites in vitro. The HIV-κ site and the c-*myc* exon and upstream sites formed complexes with identical mobilities in EMSA and B-cell nuclear extracts. As expected, the c-*myc* sites had lower affinities for the Rel family proteins. Cross-competition experiments demonstrated that each site competed with the other two for protein binding. Antibodies against Rel family members either supershifted the complexes (HIV-κ and c-*myc* exon sites) or disrupted them (c-*myc* upstream site). The explanation for this is not clear, but on the basis of the cross-competition and UV cross-linking results, we believe it is likely that Rel family proteins do recognize the c-*myc* upstream site. Other antibodies against Rel family proteins have been shown to either supershift or disrupt the EMSA complexes (23). With differentiation of pre-B 70Z/3 cells to B cells, induction of binding of nuclear factors to the c-*myc* exon and upstream elements was observed. Transfection experiments with both non-Burkitt's and Burkitt's cell lines with mutated NF-κB sites in the c-*myc* gene showed that both sites functioned as positive regulators of transcription. The decrease in promoter activity was more pronounced in the Burkitt's cell line. It is possible that the c-*myc* gene in Burkitt's cells is more dependent on the NF-κB sites. Similar NF-κB sites in the murine c-*myc* gene have been shown to function as positive transcriptional elements in murine fibroblasts and T-cell lines (12, 21). Our results demonstrate that the human c-*myc* NF-κB sites function as positive regulators of transcription in B cells.

The in vivo footprints demonstrate protection of guanine residues primarily in the 5′ half of the NF-κB sites. We find that mainly p50 binds to these sequences in vitro. There appears to be very little p65 bound to either c-*myc* site; this is most likely due to the differences from the consensus NF-κB sequence in the 3′ half of these two sites where p65 binds. Other investigators have shown, however, that there is less p65 than p50 bound to consensus NF-κB sites by using UV cross-linking analysis (10,38).

Because both of these NF-κB sites function as positive regulatory elements in transfection studies, we speculate that they are involved in the expression of the translocated c-*myc* allele in Burkitt's lymphoma cells. The sites are unoccupied in the normal c-*myc* allele, as indicated by in vivo footprinting. How access is restricted to these sites is not clear. We are investigating whether the normal allele is methylated, as a potential explanation for this phenomenon. Differences in DNase I hypersensitive sites between the translocated and the normal c-*myc* alleles in Burkitt's lymphoma cells have been found (13, 14). These results suggest that the chromatin conformation is different in each allele, and it is possible that the conformation of the normal allele prevents protein binding to the two NF-κB sites.

Deletions and mutations of the translocated c-*myc* allele in Burkitt's lymphoma are commonly seen (8, 33, 36, 37, 40). One of the two NF-κB sites has been deleted from the translocated allele of both the Raji and Ramos Burkitt's cell lines. Our transfection data suggest that a single NF-κB site is able to contribute to the transcriptional activation of the c-*myc* gene, although with the transfected construct, the level of activity is higher with two intact NF-κB sites. We have also constructed a c-*myc* promoter construct which reproduces the location of the Ramos breakpoint. The level of activity of this construct is essentially the same as that of the full-length promoter construct (data not shown). So although mutation of the upstream NF-κB site causes a substantial decrease in the level of promoter activity of the full-length construct, the level of activity of the Ramos deletion construct is higher, most likely because of the removal of several negative regulatory sites. The situation may be similar for the Raji breakpoint, although we have not tested this. The Raji breakpoint is located in a region with a negative regulatory element, but we have not mapped the relative positions of the two elements. Therefore, although the mutation of one NF-κB site causes a dramatic decrease in the level of activity in the full-length c-*myc* promoter construct, it is likely that the effect on the level of the promoter activity of the translocation breakpoints in Ramos and Raji cells is not so dramatic.

We believe that the NF-κB sites contribute to the transcriptional activity of the translocated c-*myc* allele, but it is likely that they are not the sole determinants of the transcriptional activity. We have identified other protein footprints on the translocated c-*myc* allele in addition to those reported here. It

is also likely that regulatory elements in the immunoglobulin locus play a role in expression of the translocated c-*myc* allele, perhaps both in enhancement of promoter activity and in the maintenance of an open chromatin structure. For example, it has been shown recently that increased c-*myc* expression with a shift from P2 to P1 promoter usage is observed in constructs that contain the complete immunoglobulin κ locus linked to c-*myc* (32). The constructs we used for transfection studies do not contain immunoglobulin elements, and therefore, we cannot be certain what functional role the NF-κB sites play in a model of the Burkitt's translocation. However, the fact that the NF-κB sites are occupied only in the translocated allele lends support to the idea that they play a role in the regulation of its expression.

In summary, our findings represent the first example of differential in vivo protein binding to the translocated and normal c-*myc* genes in Burkitt's cells and provide insight into the mechanism of the transcriptional regulation of the translocated c-*myc* allele.

ACKNOWLEDGMENTS

This work was supported by NIH grant CA34233 and by a grant from the Educational Foundation of America.

REFERENCES

1. **Adams, J. M., A. W. Harris, C. A. Pinkert, L. M. Corcoran, W. S. Alexander, S. Cory, R. D. Palmiter, and R. L. Brinster.** 1985. The c-*myc* oncogene driven by immunoglobulin enhancers induces lymphoid malignancy in transgenic mice. Nature (London) **318:** 533–538.
2. **Arcinas, M., and L. M. Boxer.** 1994. Differential protein binding to the c-myc promoter during differentiation of hematopoietic cell lines. Oncogene **9:**2699–2706.
3. **ar-Rushdi, A., K. Nishikura, J. Erikson, R. Watt, G. Rovera, and C. Croce.** 1983. Differential expression of the translocated and the untranslocated c-myc oncogene in Burkitt lymphoma. Science **222:** 390–393.
4. **Avigan, M. I., B. Strober, and D. Levens.** 1990. A far upstream element stimulates c-*myc* expression in undifferentiated leukemia cells. J. Biol. Chem. **265:**18538–18545.
5. **Baeuerle, P. A.** 1991. The inducible transcription activator NF-κB: regulation by distinct protein subunits. Biochim. Biophys. Acta **1072:**63–80.
6. **Battey, J., C. Moulding, R. Taub, W. Murphy, T. Stewart, H. Potter, G. Lenoir, and P. Leder.** 1983. The human c-myc oncogene: structural consequences of translocation into the IgH locus in Burkitt's lymphoma. Cell **34:**779–787.
7. **Bentley, D. L., and M. Groudine.** 1986. A block to elongation is largely responsible for decreased transcription of c-myc in differentiated HL60 cells. Nature (London) **321:**702–706.
8. **Cesarman, E., R. Dalla-Favera, D. Bentley, and M. Groudine.** 1987. Mutations in the first exon are associated with altered transcription of c-myc in Burkitt lymphoma. Science **238:**1272–1275.
9. **Chodosh, L. A.** 1988. UV crosslinking of proteins to nucleic acids, p.12.5.1–12.5.6. *In* F. M. Ausubel (ed.), Current protocols in molecular biology. Greene Publishing and Wiley-Interscience, New York.
10. **Collart, M. A., P. Baeuerle, and P. Vassalli.** 1990. Regulation of tumor necrosis factor alpha transcription in macrophages: involvement of four κB-like motifs and of constitutive and inducible forms of NF-κB. Mol. Cell. Biol. **10:**1498–1506.
11. **Cory, S.** 1986. Activation of cellular oncogenes in hemopoietic cells by chromosome translocation. Adv. Cancer Res. **47:**189–234.
12. **Duyao, M. P., A. J. Buckler, and G. E. Sonenshein.** 1990. Interaction of an NF-κB-like factor with a site upstream of the c-myc promoter. Proc. Natl. Acad. Sci. USA **87:**4727–4731.
13. **Dyson, P. J., T. D. Littlewood, A. Forster, and T. H. Rabbitts.** 1985. Chromatin structure of transcriptionally active and inactive human c-myc alleles. EMBO J. **4:**2885–2891.
14. **Dyson, P. J., and T. H. Rabbitts.** 1985. Chromatin structure around the c-myc gene in Burkitt lymphomas with upstream and downstream translocation points. Proc. Natl. Acad. Sci. USA **82:** 1984–1988.
15. **Eick, D., A. Polack, E. Kofler, and G. W. Bornkamm.** 1988. The block of elongation in c-myc exon 1 is abolished in Burkitt's lymphoma cell lines with variant translocation. Oncogene **3:**397–403.
16. **Garrity, P., and B. Wold.** 1992. Effects of different DNA polymerases in ligation-mediated PCR: enhanced genomic sequencing and in vivo footprinting. Proc. Natl. Acad. Sci. USA **89:**1021–1025.
17. **Gauss, G. H., and M. R. Lieber.** 1992. DEAE-dextran enhances electroporation of mammalian cells. Nucleic Acids Res. **20:**6739–6740.
18. **Gorman, C. M., L. F. Moffat, and B. H. Howard.** 1982. Recombinant genomes which express chloramphenicol acetyltransferase in mammalian cells. Mol. Cell. Biol. **2:**1044–1051.
19. **Hayday, A. C., S. D. Gillies, H. Saito, C. Wood, D. Wiman, W. S. Hayward, and S. Tonegawa.** 1984. Activation of a translocated human c-myc gene by an enhancer in the immunoglobulin heavy-chain locus. Nature (London) **307:**334–340.
20. **Higuchi, R.** 1990. Recombinant PCR, p. 177–183. *In* M. A. Innis, D. M. Gelfand, J. J. Sninsky, and T. J. White (ed.), PCR protocols: a guide to methods and applications. Academic Press, Inc., San Diego, Calif.
21. **Kessler, D. J., D. B. Spicer, F. A. La Rosa, and G. Sonenshein.** 1992. A novel NF-κB element within exon 1 of the murine c-*myc* gene. Oncogene **7:**2447–2453.
22. **La Rosa, F. A., J. W. Pierce, and G. E. Sonenshein.** 1994. Differential regulation of the c-*myc* oncogene promoter by the NF-κB Rel family of transcription factors. Mol. Cell. Biol. **14:** 1039–1044.
23. **Liou, H.-C., W. C. Sha, M. L. Scott, and D. Baltimore.** 1994. Sequential induction of NF-kB/Rel family proteins during B-cell terminal differentiation. Mol. Cell. Biol. **14:**5349–5359.
24. **Lombardi, L., E. W. Newcomb, and R. Dalla-Favera.** 1987. Pathogenesis of Burkitt lymphoma: expression of an activated c-myc oncogene causes the tumorigenic conversion of EBV-infected human B lymphoblasts. Cell. **49:**161–170.
25. **Maxam, A. M., and W. Gilbert.** 1980. Sequencing end-labeled DNA with base-specific chemical cleavages. Methods Enzymol. **65:**499–560.
26. **Mueller, P. R., and B. Wold.** 1989. In vivo footprinting of a muscle specific enhancer by ligation-mediated PCR. Science **246:**780–786.
27. **Nepveu, A., and K. B. Marcu.** 1986. Intragenic pausing and antisense transcription within the murine c-myc locus. EMBO J. **5:** 2859–2865.
28. **Nishikura, K., A. ar-Rushdi, J. Erikson, R. Watt, G. Rovera, and C. M. Croce.** 1983. Differential expression of the normal and of the translocated human c-myc oncogenes in B cells. Proc. Natl. Acad. Sci. USA **80:**4822–4826.
29. **Nussenzweig, M. D., E. Schmidt, A. C. Shaw, E. Sinn, J. Campos-Torres, B. Mathey-Prevot, P. K. Pattengale, and P. Leder.** 1988. A human immunoglobulin gene reduces the incidence of lymphomas in c-*myc*-bearing transgenic mice. Nature (London) **336:**446–450.
30. **Pelicci, P. G., D. M. Knowles, I. Magrath, and R. Dalla-Favera.** 1986. Chromosomal breakpoints and structural alterations of the c-myc locus differ in endemic and sporadic forms of Burkitt lymphoma. Proc. Natl. Acad. Sci. USA **83:**2984–2988.
31. **Pfeifer, G. P., S. D. Steigerwald, P. R. Mueller, B. Wold, and A. D. Riggs.** 1989. Genomic sequencing and methylation analysis by ligation mediated PCR. Science **246:**810–813.
32. **Polack, A., R. Feederle, G. Klobeck, and K. Hortnagel.** 1993. Regulatory elements in the immunoglobulin kappa locus induce c-myc activation and the promoter shift in Burkitt's lymphoma cells. EMBO J. **12:**3913–3920.
33. **Rabbitts, T. H., A. Forster, P. Hamlyn, and R. Baer.** 1984. Effect of somatic mutation within translocated c-myc genes in Burkitt's lymphoma. Nature (London) **309:**592–597.
34. **Saluz, H. P., and J. P. Jost.** 1987. A laboratory guide to genomic sequencing. Birkhauser, Boston.
35. **Sen, R., and D. Baltimore.** 1986. Inducibility of κ immunoglobulin enhancer-binding protein NF-κB by a posttranslational mechanism. Cell **47:**921–928.

36. **Siebenlist, U., L. Henninghausen, J. Battey, and P. Leder.** 1984. Chromatin structure and protein binding in the putative regulatory region of the c-myc gene in Burkitt lymphoma. Cell. **37:**381–391.
37. **Taub, R., C. Moulding, J. Battey, W. Murphy, T. Vasicek, G. M. Lenoir, and P. Leder.** 1984. Activation and somatic mutation of the translocated c-myc gene in Burkitt lymphoma cells. Cell **36:** 339–348.
38. **Urban, M. B., R. Schreck, and P. A. Baeuerle.** 1991. NF-κB contacts DNA by a heterodimer of the p50 and p65 subunit. EMBO J. **10:**1817–1825.
39. **Wijnholds, J., J. N. Philipsen, and G. Ab.** 1988. Tissue-specific and steroid-dependent interaction of transcription factors with the oestrogen-inducible apoVLVL II promoter in vivo. EMBO J. **7:**2757–2763.
40. **Yu, B. W., I. Ichinose, M. A. Bonham, and M. Zajac-Kaye.** 1993. Somatic mutations in c-*myc* intron I cluster in discrete domains that define protein binding sequences. J. Biol. Chem. **268:**19586–19592.
41. **Zajac-Kaye, M., E. P. Gelmann, and D. Levens.** 1988. A point mutation in the c-myc locus of a Burkitt lymphoma abolishes binding of a nuclear protein. Science **240:**1776–1780.